# Measurement of the $pd \to pd\eta$ cross section in complete kinematics

R. Bilger,[1] W. Brodowski,[1] H. Calén,[2] H. Clement,[1] C. Ekström,[2] G. Fäldt,[3] K. Fransson,[3] L. Gustafsson,[3] B. Höistad,[3] A. Johansson,[3] T. Johansson,[3] K. Kilian,[4] S. Kullander,[3] A. Kupsc,[2] G. Kurz,[1] P. Marciniewski,[3] B. Morosov,[5] A. Mörtsell,[3] W. Oelert,[4] V. Renken,[4] R. Ruber,[2] B. Shwartz,[7] V. Sopov,[6] J. Stepaniak,[8] A. Sukhanov,[5] P. Thörngren-Engblom,[3] A. Turowiecki,[9] G. J. Wagner,[1] Z. Wilhelmi,[9] C. Wilkin,[10] J. Zabierowski,[11] and J. Złomańczuk[3,*]

[1]*Physikalisches Institut, Tübingen University, D-72076 Tübingen, Germany*

[2]*The Svedberg Laboratory, S-751 21 Uppsala, Sweden*

[3]*Department of Radiation Sciences, Uppsala University, S-751 21 Uppsala, Sweden*

[4]*IKP - Forschungszentrum Jülich GmbH, D-52425 Jülich, Germany*

[5]*Joint Institute for Nuclear Research Dubna, 101000 Moscow, Russia*

[6]*Institute of Theoretical and Experimental Physics, 117259 Moscow, Russia*

[7]*Budker Institute of Nuclear Physics, Novosibirsk 630 090, Russia*

[8]*Soltan Institute for Nuclear Studies, PL-00681 Warsaw, Poland*

[9]*Institute of Experimental Physics, Warsaw University, PL-00681 Warsaw, Poland*

[10]*Physics and Astronomy Department, UCL, London WC1E 6BT, United Kingdom.*

[11]*Soltan Institute for Nuclear Studies, PL-90137 Łódz, Poland*

(Received 6 October 2003; published 28 January 2004)

The $pd \to pd\eta$ reaction has been studied in a kinematically complete experiment at five beam energies 927, 961, 996, 1032, and 1096 MeV. In contrast to our measurement of the $pd \to {}^3\mathrm{He}\,\eta$ at the same energies, all the c.m. angular distributions are consistent with isotropy. The energy dependence of the total cross section seems to follow a three-body phase space as modified by a proton-deuteron final-state interaction, and such an extrapolation is consistent with other near-threshold data. The distributions of the $pd$ and $p\eta$ invariant mass at fixed beam energy are both close to those of phase space. However, this is not the case for the $d\eta$ invariant mass, which shows significant structure in the first few MeV above threshold. This behavior is similar to that observed in the energy variation of the $pn \to d\eta$ total cross section and is the sign of a large $\eta$-deuteron scattering length that has been predicted in many theoretical models.

DOI: 10.1103/PhysRevC.69.014003 PACS number(s): 25.40.Ve, 25.10.+s

## I. INTRODUCTION

The threshold enhancements in reactions leading to the ${}^3\mathrm{He}\,\eta$ [1,2] and ${}^4\mathrm{He}\,\eta$ [3,4] final states clearly show the low energy $\eta$-nucleus interaction to be strong and attractive. These enhancements might turn out to be signals for $\eta$-nucleus quasibound states [5] that were first predicted for somewhat heavier nuclei [6]. To investigate this possibility further, data are required for other nuclei. The $\eta$-deuteron system is of particular interest because the three-body system can be studied reliably using the Faddeev equations and striking phenomena had been foreseen there [7].

Due to isospin conservation, the $d\eta$ final state is not directly accessible in pion-deuteron scattering and the coherent $\gamma d \to d\eta$ reaction is suppressed by the weak coupling of isoscalar photons to the $N^*(1535)$ resonance [8], a state that is expected to dominate low energy $\eta$ production. Other entrance channels must therefore be found to produce the $d\eta$ system.

An inclusive measurement of the $p(n,d)X$ reaction with a broad-band neutron beam [9] was subsequently interpreted as showing evidence for the $np \to d\eta$ two-body reaction [10]. These authors concluded that there was a very strong $d\eta$ final-state interaction (fsi). The same reaction has been studied through quasifree production on a deuterium target over a wide range of c.m. energies by determining the $\eta$ momentum and deuteron direction [11]. Very close to threshold the recoil deuteron momentum was measured in a small spectrometer with a resolution in c.m. excess energy, $Q = \sqrt{s} - \Sigma_f m_f$, of the order of 1 MeV over a narrow range in $Q$ [12]. Despite relatively large statistical errors, these data indicated a significant $d\eta$ threshold enhancement, though not as big as that of the earlier claim [10].

In an alternative experimental approach, the $d\eta$ system can be produced in a three-body final state, for example, through the $pd \to pd\eta$ reaction. The process has been studied very close to threshold by detecting the final proton and deuteron, but only total cross sections could be extracted [13]. Furthermore, at such low energies the phase space is small and the range of accessible $d\eta$ excitation energies $Q_{d\eta}$ very limited. This can be overcome by working at slightly higher energies, as we did when measuring the $pd \to {}^3\mathrm{He}\,\eta$ reaction [14]. The two-body reaction can be thought of as the kinematic limit of $pd \to pd\eta$, where the proton-deuteron fsi has caused these particles to fuse to form the observed ${}^3\mathrm{He}$ nucleus. Such a picture allows one to make simple estimates for one cross section in terms of the other [15]. It also suggests that the same dynamical mechanism is likely to be the main driving term for both reactions, perhaps involving the production of a pion on one of the target nucleons which is converted into the observed $\eta$ meson through an interaction on the second target nucleon [16–19].

*Email address: jozef.zlomanczuk@tsl.uu.se

 

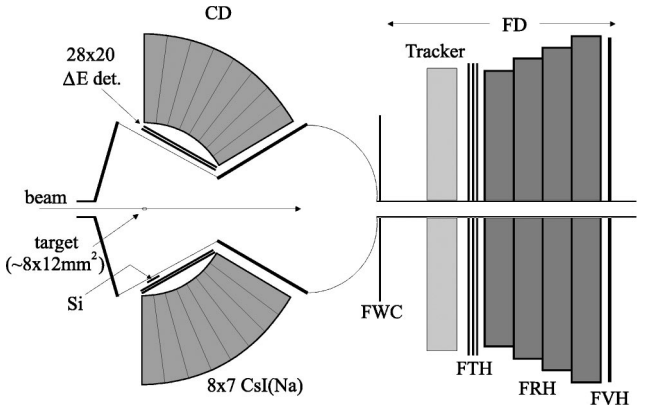


FIG. 1. Schematic representation of the PROMICE-WASA setup.

## II. APPARATUS

The experiment was carried out at the CELSIUS storage ring of The Svedberg Laboratory, Uppsala, using the WASA/PROMICE experimental apparatus. Since the setup was identical to that used for the $pd \rightarrow {}^3\mathrm{He}\,\eta$ reaction, run in parallel [14], only the principal elements will be discussed here.

The $\eta$ meson could be detected directly through its $2\gamma$ decay mode, with the photons registered in the central detector (CD), consisting of two arrays of CsI crystals preceded by veto counters, as illustrated in Fig. 1. All protons and deuterons produced in the $pd \rightarrow pd\,\eta$ reaction at our beam energies, except for those lost down the beam pipe ($\theta < 4.5°$), fall within the angular acceptance of the forward detector (FD). In the FD, in addition to the tracker, there are four sets of scintillators. Of particular importance here are the forward trigger hodoscopes (FTH) and forward range hodoscopes (FRH) consisting of three 5 mm thick layers and four 11 cm layers, respectively, which are vital for particle identification and energy determination.

## III. PARTICLE IDENTIFICATION AND BEAM ENERGY DETERMINATION

The signal for the reaction is two charged particles in the forward detector in association with two neutral hits in the central detector. It is first necessary to make sure that the charged particles correspond to a proton-deuteron pair. Particle identification is established through the correlation between energy losses in the adjacent layers of the FD. As an example, the energy loss in the last layer of the FTH vs the energy deposited by the particle stopped in the first layer of the FRH is shown in Fig. 2. The bands corresponding to protons and deuterons are clearly identified and these are well separated from that associated with $^3$He.

Our measurement of the $pd \rightarrow {}^3\mathrm{He}\,\eta$ reaction [14] was carried out well above threshold and, for this purpose, the determination of the beam momentum from the radio frequency and the nominal circumference of the accelerator was quite sufficient. This is no longer the case with the present experiment since any uncertainty here also contributes to the errors in the missing mass, which are of particular significance in the $d\,\eta$ threshold region.

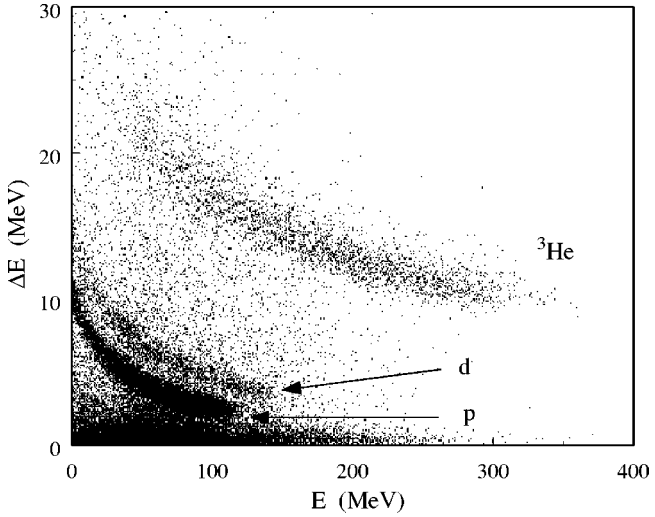


FIG. 2. $\Delta E$-$E$ plot showing bands corresponding to protons, deuterons, and $^3$He identified in the forward detector.

In order to minimize the beam energy uncertainty, we have reanalyzed our $pd \rightarrow {}^3\mathrm{He}\,\eta$ data and fixed the value of the beam energy by looking at the correlation between the energy and angle of the recoil $^3$He, as illustrated at the *nominal* energy of 1037 MeV in Fig. 3. It should be noted that for such a two-body reaction the maximum production angle

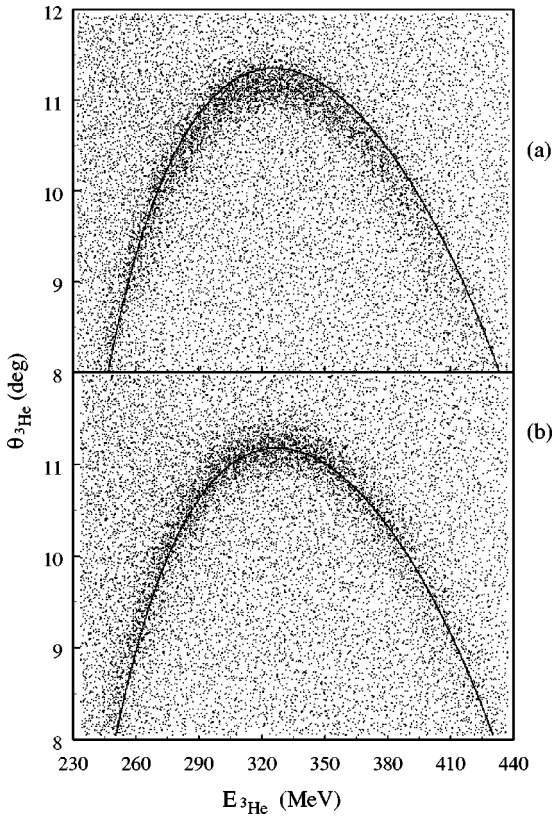


FIG. 3. Two-dimensional scatter-plot of $^3$He angle vs kinetic energy for the *nominal* beam energy of 1037 MeV, compared to the two-body kinematical curves calculated for the beam energies of 1037 MeV (a) and 1032 MeV (b). The value $m_\eta = 547.3\ \mathrm{MeV}/c^2$ [21] is assumed.

depends only upon the beam energy. The curve, corresponding to the nominal energy of 1037 MeV and a meson mass $m_\eta = 547.3$ MeV/$c^2$ [21], does not reproduce well the maximum angle; the 1032 MeV curve gives a much better fit to the experimental distribution. The *true* beam energies can be determined in this way to ±1 MeV, and this is consistent with the best fits at all energies giving reductions of between 3 and 5 MeV in the nominal figures. Such changes are compatible with the uncertainty in the true circumference of the beam circulating within the machine ring. We have therefore used the adjusted values of 927, 961, 1032, and 1096 MeV, in both the analysis of the experimental data and in the Monte Carlo simulation, rather than the nominal ones quoted in Ref. [14].

## IV. DATA ANALYSIS

Having identified the proton-deuteron pair using the $\Delta E$-$E$ plot of Fig. 2, the major difficulty in measuring the $pd \rightarrow pd\eta$ reaction is the huge background coming from other $pdX$ channels. The $\eta$ peak is clearly seen in the proton-deuteron missing mass distribution, $MM_{pd}$, at all energies; the 1032 MeV results are shown in Fig. 4. However, the peak represents only a tiny fraction of the total events and differential cross sections extracted from such data would suffer from prohibitively large errors arising from the background subtraction.

The background is greatly reduced if photons from $\pi^0$ and $\eta$ decays are measured in coincidence. The lower part of Fig. 4 presents the correlation between $MM_{pd}$ and the two-photon invariant mass $M_{\gamma\gamma}$ obtained at 1032 MeV. The $\eta$ island, where the $pd \rightarrow pd\eta$ reaction is identified through both the $\eta$ invariant and missing mass peaks, is well separated from the single and multipion production regions. There is also strong evidence for $\eta$ decay into the three-pion channels, but the major background comes from the combinatorial background where two photons from different $\pi^0$, in say $\eta \rightarrow \pi^0\pi^0\pi^0$ or $pd \rightarrow pd\pi^0\pi^0$, are observed in the CD.

By imposing the cut $M_{\gamma\gamma} > 450$ MeV/$c^2$, we only use data from the $\eta$-island region in our extraction of the $pd \rightarrow pd\eta$ channel. This is at the expense of a large reduction in statistics caused by the limited solid angle of our photon detectors. The $MM_{pd}$ distributions obtained at different energies are compared in Fig. 5 to the phase-space Monte Carlo simulation of the $pd \rightarrow pd\eta$ reaction. The tails of the $\eta$ peaks are reasonably well reproduced, suggesting that we have a nearly background-free sample of $pd \rightarrow pd\eta$ events.

The momenta of the photons from the $\eta$ decay are measured with much poorer resolution than those of the protons and deuterons. The resolution in the directly measured $d$-$\eta$ invariant mass $M_{d\eta}$ is therefore much worse than that in the missing mass calculated using the four-momentum of the detected proton $MM_p$, to which it should be kinematically identical. Though the uncertainty in the beam energy also contributes to errors in the $MM_p$ determination, it is used here as the best estimate of $M_{d\eta}$.

## V. RESULTS

As can be seen from the 1032 MeV data shown in Fig. 6, the phase-space Monte Carlo reproduces reasonably well the angular distributions measured for the three final-state particles. The Monte Carlo may therefore be used to evaluate the detector acceptance and thus correct the experimental distributions. The c.m. angular distributions obtained at 1032 MeV and corrected for acceptance are shown in Fig. 7. At this, and all the other energies, the $\eta$ c.m. angular distributions are consistent with isotropy and this is in marked contrast to the angular variation seen in the $pd \rightarrow {}^3\mathrm{He}\,\eta$ case, where the cross sections are all maximal around $\cos\theta_\eta \approx 0.5$ [14]. Slight deviations from isotropy might be present in the proton distribution but any such effect is marginal.

The distributions have been normalized by comparing the total number of $pd \rightarrow pd\eta$ events to those of the $pd \rightarrow {}^3\mathrm{He}\,\eta$ reaction measured in parallel under the same conditions, i.e., with the requirement that both photons from the $\eta$ decay were detected in the CD. These numbers were obtained by taking the $\eta$-peak areas in the $MM_{pd}$ and $MM_{^3\mathrm{He}}$ distributions and correcting them for acceptance. The $pd \rightarrow {}^3\mathrm{He}\,\eta$ cross sections were taken from Ref. [14], with the value at 996 MeV, where the luminosity was uncertain, being found by interpolating between the 966 and 1032 MeV points.

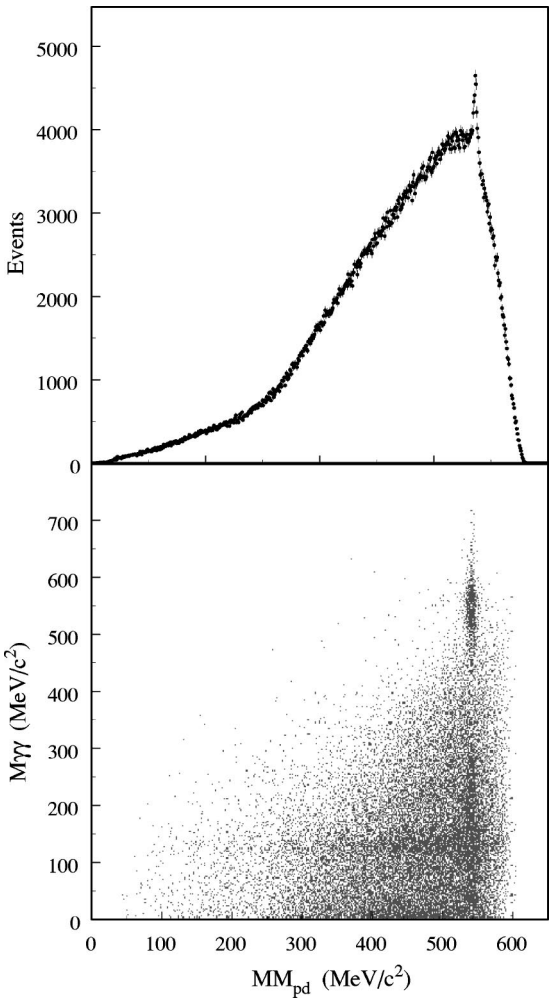


FIG. 4. Upper frame: Missing mass distribution for detected proton-deuteron pairs. Lower frame: Correlation between the missing mass $MM_{pd}$ and the two-photon invariant mass $M_{\gamma\gamma}$ obtained at 1032 MeV showing the island of well-identified $pd\eta$ events.

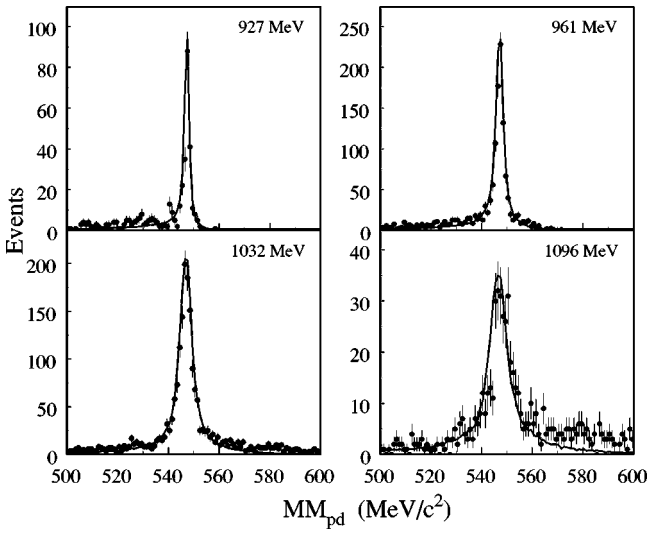


FIG. 5. Comparison between the experimental missing mass distributions (points) obtained at our four energies for $M_{\gamma\gamma} > 450$ MeV/$c^2$ to the distributions obtained in the phase-space Monte Carlo simulation of the $pd \rightarrow pd\eta$ reaction (curves).

Simulations of the detector response were carried out with the GEANT 3.21 and GHEISHA programs [20]. Though these are tuned for higher energy particles, we have checked that nuclear interactions of deuterons in plastic scintillator are reproduced to within 20% in our energy range. Such uncertainties in the rate of nuclear interactions introduce systematic errors in the final cross sections varying from 10% at 927 MeV to 17% at 1096 MeV. To these must be added the overall normalization error of 20% quoted for the $pd \rightarrow {}^3\mathrm{He}\,\eta$ reaction [14].

The total cross sections, obtained by integrating the differential cross sections, are listed in Table I and shown as a function of the overall excess energy $Q$ in Fig. 8, together with the very low energy Saclay data [13].

If one neglects the final rescattering of the $\eta$ then, at low energies, one would expect the total cross section to vary as [15]

$$\sigma_T = C\frac{(Q/\epsilon)^2}{(1+\sqrt{1+Q/\epsilon})^2}. \qquad (1)$$

Here $\epsilon$ is the energy of the $S$-wave $pd$ bound state in the spin doublet, or virtual state in the quartet, and $C$ is approximately constant. Taking $\epsilon = 5.5$ MeV and $C = 350$ nb leads to the curve, shown in the figure, which links our points to those of Saclay [13]. If there is a $pd\eta$ enhancement to parallel that of $pd \rightarrow {}^3\mathrm{He}\,\eta$ at low $Q$ [2] then it would require a much more detailed scan of the near-threshold region to establish it.

The two-dimensional plot of $M_{pd}$ vs $M_{d\eta}$ is shown in Fig. 9 for the 1032 MeV data set. There is evidence for an excess of points at low $M_{d\eta}$ but nothing significant in the other two invariant masses. This behavior is confirmed in the one-dimensional projections of the plots shown in Fig. 10 at the same energy.

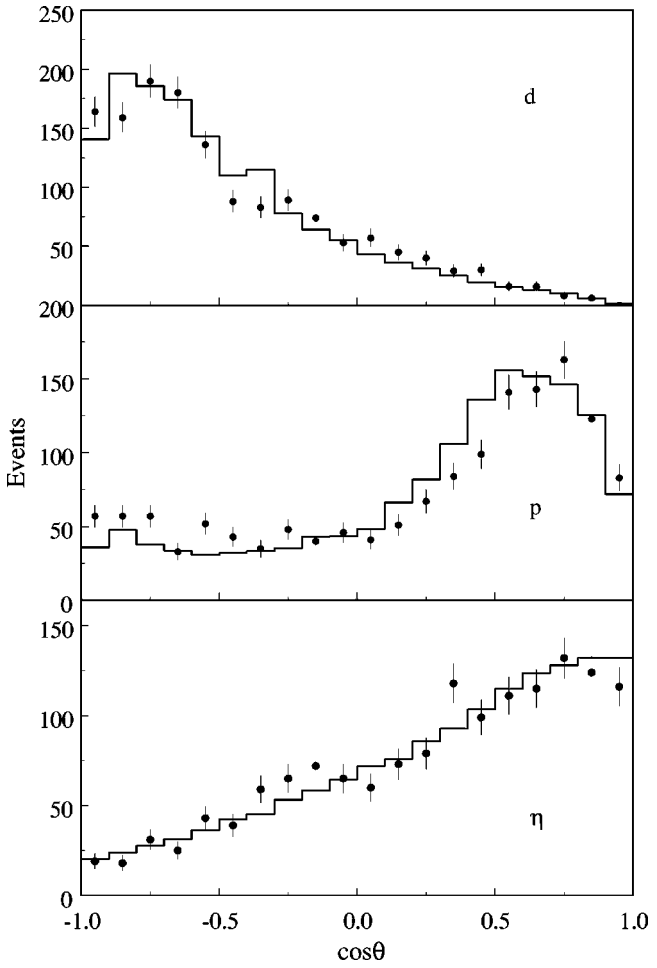


FIG. 6. Raw distributions in the cosine of the c.m. angle of deuterons (upper), protons (middle), and $\eta$ mesons (lower frame) for the 1032 MeV data compared to the results of phase-space Monte Carlo simulations assuming isotropic distributions.

As well as displaying flat angular distributions, the $pd$ and $p\eta$ invariant mass distributions are also consistent with the phase-space predictions that are shown in Fig. 10. Phase space does not reproduce the $d\eta$ effective mass spectrum, where there is an excess of events at low $M_{d\eta}$. The ratio of this to phase space, arbitrarily normalized, is shown in Fig. 11 as a function of the $d\eta$ excitation energy $Q_{d\eta} = M_{d\eta} - m_d - m_\eta$ for the 1032 MeV data. There is in fact an enhancement for $Q_{d\eta} \leqslant 10$ MeV at all beam energies, but it is seen most clearly at 1032 MeV, where the Dalitz plot has opened out but where the resolution in $Q_{d\eta}$ is still very good. It is important in this context to note that an uncertainty of ±1 MeV in beam energy translates to just over half this value in $Q_{d\eta}$.

If the enhancement seen in Fig. 11 is a property of the final $d\eta$ system then it should be seen for other entrance channels. The only one for which there are reasonable data is the $pn \rightarrow d\eta$ reaction [11]. The values of the total cross section divided by the phase-space factor of $\sqrt{Q_{d\eta}}$ also show a consistent threshold enhancement with a width of a few MeV, as illustrated in Fig. 11. Although the relative normalization is arbitrary, the shapes of the two distributions certainly give consistent hints of a strong $\eta d$ final-state inter-

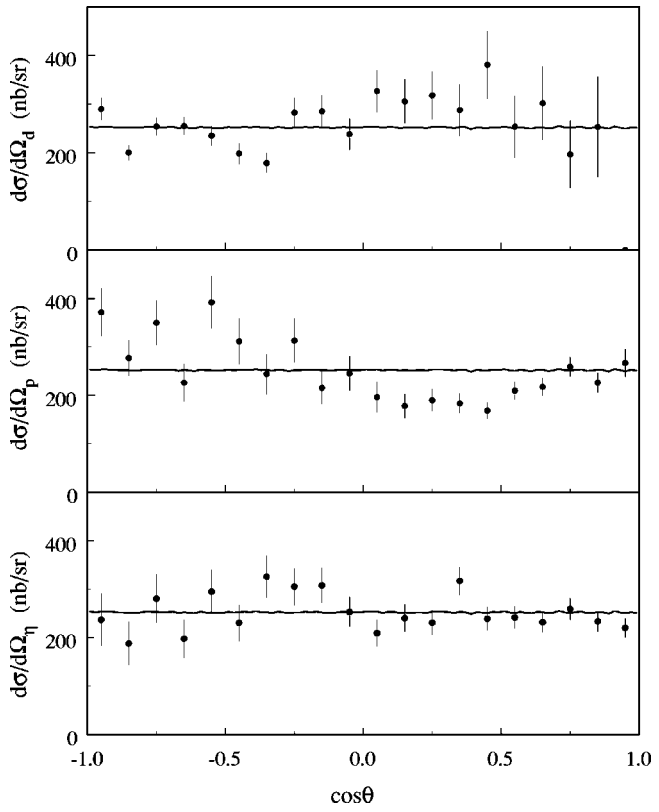


FIG. 7. Acceptance-corrected distributions in the cosine of the c.m. angle of deuterons (upper), protons (middle), and $\eta$ mesons (lower frame) for the 1032 MeV data.

action. Our results at other energies are consistent with this shape, though with larger error bars, especially in the crucial small $Q_{d\eta}$ region.

## VI. COMPARISON WITH THEORY

The final *pd* spin-doublet contribution to the value of $C$ in Eq. (1) can be estimated from final-state interaction theory in terms of $pd \to {}^3\mathrm{He}\,\eta$ data [15]. At low energies one then expects that

TABLE I. Total cross section for the $pd \to pd\eta$ reaction. In addition to the statistical errors quoted, there is an overall normalization uncertainty of about 20%, arising from that in the $pd \to {}^3\mathrm{He}\ \eta$, and an effect due to interactions of particles in the detectors, which increases over our energy range from 10% to 17%. The ±1 MeV uncertainty in the beam energy corresponds to one of ≈±0.55 MeV in $Q$.

| $T_p$(MeV) | $Q$(MeV) | $\sigma_T(\mu\mathrm{b})$ |
|---|---|---|
| 927 | 14.5 | 0.26±0.02 |
| 961 | 33.3 | 0.80±0.04 |
| 996 | 52.5 | 2.0±0.1 |
| 1032 | 72.3 | 3.0±0.2 |
| 1096 | 107.1 | 5.2±0.6 |

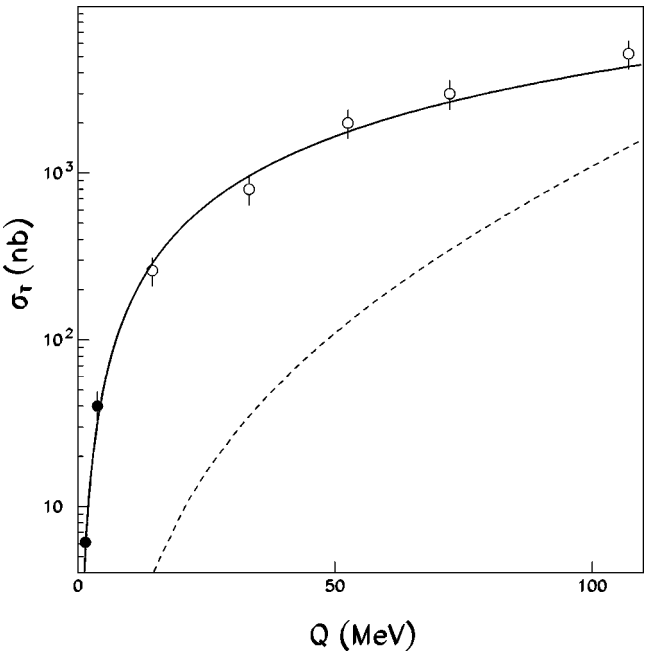


FIG. 8. Total cross section of the $pd \to pd\eta$ reaction as a function of the excess energy $Q$. The empty circles represent results of this work and the full circles are taken from Ref. [13]. The solid curve has been calculated using Eq. (1) with $C$ being taken as constant. The dashed curve is the single scattering approximation obtained by smearing the measured $pn \to d\eta$ cross section [11] over the neutron Fermi momentum.

$$C_2 \approx \frac{1}{4}\left(\frac{\epsilon}{Q}\right)^{1/2} \sigma_T(pd \to {}^3\mathrm{He}\,\eta). \tag{2}$$

Since the $pd \to {}^3\mathrm{He}\,\eta$ results show a strong threshold enhancement [2], whereas the combination of data in Fig. 8 does not, this formula would demand that $C_2$ varies fast with $Q$. Nevertheless, if we use the threshold $pd \to {}^3\mathrm{He}\,\eta$ data, we obtain a value $C_2 \approx 450$ nb, which is in very satisfactory agreement with the 350 nb used to produce the curve of Fig. 8. The contradiction in the $Q$ dependence

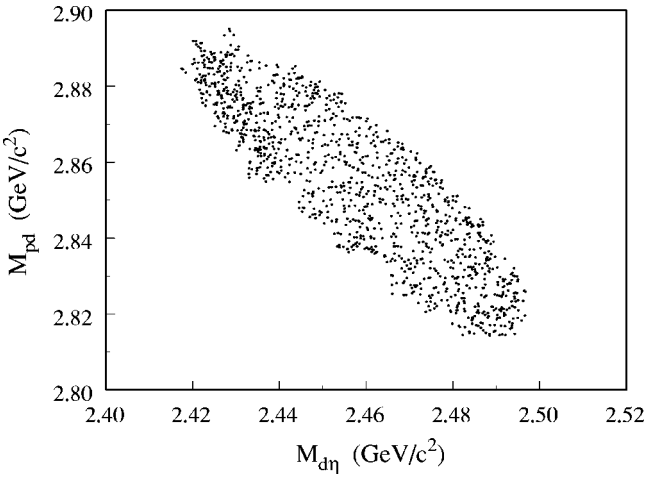


FIG. 9. Two-dimensional plot of $M_{pd}$ vs $M_{d\eta}$ at 1032 MeV.

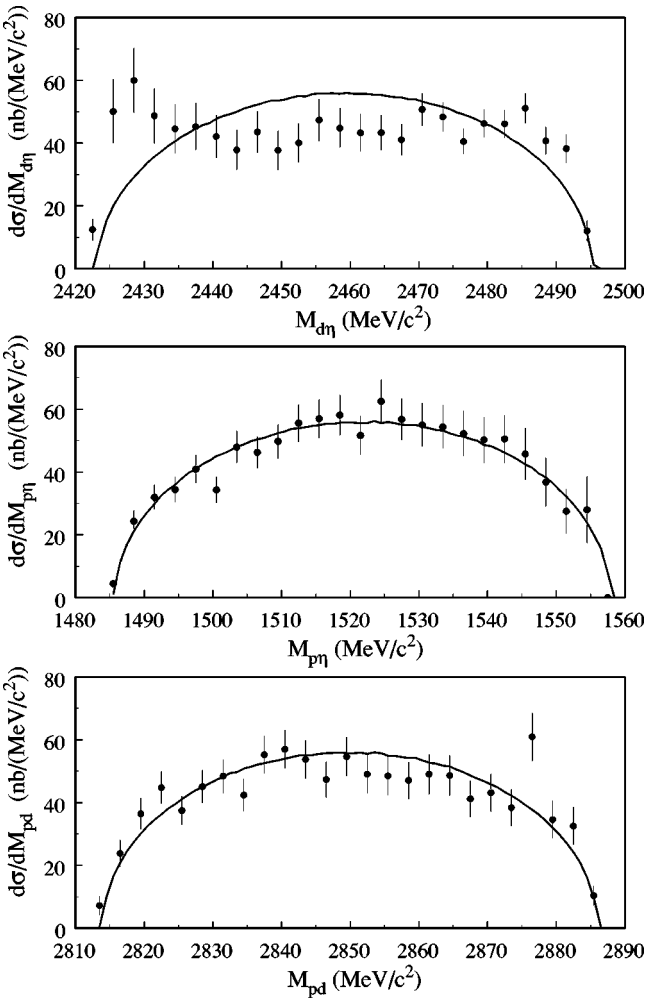


FIG. 10. One-dimensional distributions in the three final-state effective masses compared to phase-space predictions at a beam energy of 1032 MeV. Note the excess of events at low $M_{d\eta}$.

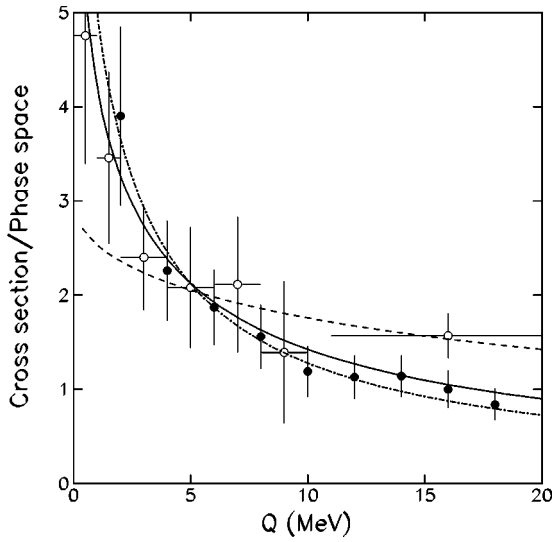


FIG. 11. Ratio of the cross section for the production of the $d\eta$ system to arbitrarily normalized phase space, as a function of the kinetic energy in the $d\eta$ rest frame, for the $pn \to d\eta$ total cross section (open circles) [11] and for the $pd \to pd\eta$ reaction at 1032 MeV (closed circles) [this work]. The broken, solid, and chain curves are the predictions of the scattering length formula of Eq. (3) using as input $a(d\eta) = (0.73 + 0.56i)$ fm, $(1.64 + 2.99i)$ fm, and $(-4.69 + 1.59i)$ fm, respectively [23]. In all cases the overall normalization is arbitrary.

may arise from the assumption made in Ref. [15] that only the $pd$ interaction is significant in the final state.

The theory of the low energy $d\eta$ system has been studied by many authors using a variety of approximations in the three-body scattering equations [7,22–27]. Though some of the results are different, even for the same basic input, the major uncertainty in the predictions arises from the poor knowledge of the $\eta$-nucleon low energy parameters which are the essential ingredients of any of the calculations. Whereas the imaginary part of the $\eta$-nucleon scattering length $a(N\eta)$ is thought to be in the 0.25–0.35 fm range, estimates of the real part between 0.25 and 0.98 fm follow from multiresonance fits [28] and values even outside this range are to be found in the literature [29,30]. Provided that $\mathrm{Re}\{a(N\eta)\} \gtrsim 0.5$ fm, the models generally predict very strong $\eta$-deuteron scattering lengths $a(d\eta)$.

If only the scattering length contribution is kept, the amplitude squared for the production of a $d\eta$ system at low relative momentum $k$ should be proportional to

$$|F(k)|^2 = \frac{N}{|1 - ika(d\eta)|^2} = \frac{N}{[1 + \mathrm{Im}\{a(d\eta)\}]^2 + [k\ \mathrm{Re}\{a(d\eta)\}]^2}, \tag{3}$$

where $N$ is a scale factor that depends upon the particular reaction studied.

Purely for the sake of definiteness we take the evaluations of Shevchenko *et al.* [23] where, for $a(N\eta) = (0.25 + 0.16i)$ fm, $(0.55 + 0.30i)$ fm, and $(0.98 + 0.37i)$ fm, they obtain $a(d\eta) = (0.73 + 0.56i)$ fm, $(1.64 + 2.99i)$ fm, and $(-4.69 + 1.59i)$ fm, respectively. In the last case the interaction is so strong that $\mathrm{Re}\{a(d\eta)\}$ has changed sign and the system is in the quasibound-state regime [7]. The shapes then predicted by Eq. (3) for these three values of the $d\eta$ scattering length are shown in Fig. 11. It is clear that our results do not favor the weak scattering length prediction, $(0.73 + 0.56i)$ fm but, by themselves, the data are completely insensitive to the sign of $\mathrm{Re}\{a(d\eta)\}$ and so cannot distinguish between the other two solutions shown, i.e., whether there is a quasibound $d\eta$ state or not.

The only microscopic estimate of the near-threshold $pd \to pd\eta$ reaction was made by Tengblad [20] in a model where a pion is first produced through the $pp \to d\pi^+$ reaction on the proton in the deuteron target and the observed $\eta$ produced through the $\pi^+ n \to p\eta$ reaction on the neutron in the deuteron target. Such a model describes well the near-threshold $pd \to {}^3\mathrm{He}\,\eta$ reaction once the $\eta$ rescattering has been incorporated [17]. Although the Tengblad predictions

fall only a little below the results of the near-threshold data [13], the final-state interactions in neither the $pd$ nor $d\eta$ systems were taken into account. On the other hand, she argued that for higher beam energies, as one approaches the free $pn \to d\eta$ threshold at 1250 MeV ($Q \approx 190$ MeV), the pole term involving quasifree $\eta$ production on the neutron should be dominant. As can be seen from the estimate shown by the dashed curve in Fig. 8, obtained using the Paris deuteron wave function [31], such a contribution already provides about one third of the total cross section for our 1096 MeV data. It is therefore likely that our data span a region where both quasifree and two-step production are important.

## VII. SUMMARY

In summary, we have made a kinematically complete measurement of the $pd \to pd\eta$ reaction away from threshold. The angular distributions are consistent with $S$-wave dominance in the final state and the energy variation of the total cross section follows closely that predicted by final-state-interaction theory where the $\eta$ rescattering is neglected. The cross section normalization is close to that determined from the threshold $pd \to {}^3\mathrm{He}\,\eta$ data. More theoretical work is, however, needed here in view of the lack of an evident threshold enhancement in the low energy $pd \to pd\eta$ data, though these are of limited quality.

For excess energies above 200 MeV we would expect the $pd \to pd\eta$ reaction to be completely dominated by quasifree $pn \to d\eta$ production on a neutron in the deuteron, leaving a proton spectator. Our estimates suggest that at the energy of 1096 MeV the quasifree contribution should still represent about a third of the total cross section. The fraction drops to the order of one percent at the lowest energy indicating that other mechanisms, where there is no spectator proton, are also necessary. The most credible of these involves the production of an intermediate virtual pion.

We also find a strong final-state interaction peak in the $d\eta$ system, which is the sign of a large $d\eta$ scattering length. Though this is in agreement with the existing $pn \to d\eta$ total cross section data, the 1032 MeV results allow us to quantify the effect more precisely.

The results are very germane to the ongoing discussion of the possible existence of $\eta$ nuclei. The strong $d\eta$ scattering length indicated by our experiment implies a large real part in the $\eta$-nucleon scattering length. This means that it is then highly likely that the $\eta$ would form a quasibound state with one of the helium isotopes, where the numbers of nucleons are higher and the system is more compact.

## ACKNOWLEDGMENTS

The support of the TSL/ISV personnel during the course of this work was invaluable. Financial backing for this experiment and its analysis was provided by the Swedish Natural Science Research Council, the Swedish Royal Academy of Science, the Swedish Institute, Deutsche Forschung Gesellschaft (Mu 705/3 Graduiertenkolleg), the Polish Scientific Research Committee, the Russian Academy of Science, the German Bundesministerium für Bildung und Forschung [06TU886 and DAAD], and the European Science Exchange Program.

[1] J. Berger *et al.*, Phys. Rev. Lett. **61**, 919 (1988).
[2] B. Mayer *et al.*, Phys. Rev. C **53**, 2068 (1996).
[3] R. Frascaria *et al.*, Phys. Rev. C **50**, R537 (1994).
[4] N. Willis *et al.*, Phys. Lett. B **406**, 143 (1997).
[5] C. Wilkin, Phys. Rev. C **47**, R938 (1993).
[6] Q. Haider and L. C. Liu, Phys. Lett. B **172**, 257 (1986).
[7] T. Ueda, Phys. Rev. Lett. **66**, 297 (1991); Phys. Scr. **48**, 68 (1993).
[8] B. Krusche *et al.*, Phys. Rev. Lett. **74**, 3736 (1995).
[9] F. Plouin *et al.*, Nucl. Phys. **A302**, 413 (1978).
[10] F. Plouin, P. Fleury, and C. Wilkin, Phys. Rev. Lett. **65**, 690 (1990).
[11] H. Calén *et al.*, Phys. Rev. Lett. **79**, 2642 (1997).
[12] H. Calén *et al.*, Phys. Rev. Lett. **80**, 2069 (1998).
[13] F. Hibou *et al.*, Eur. Phys. J. A **7**, 537 (2000).
[14] R. Bilger *et al.*, Phys. Rev. C **65**, 044608 (2002).
[15] G. Fäldt and C. Wilkin, Phys. Lett. B **382**, 209 (1996).
[16] K. Kilian and H. Nann, in *Particle Production Near Threshold*, edited by Hermann Nann and Edward J. Stephenson, AIP Conf. Proc. No. 221 (AIP, New York, 1991), p. 185.
[17] G. Fäldt and C. Wilkin, Nucl. Phys. **A587**, 769 (1995).
[18] J. Złomańczuk *et al.*, Acta Phys. Pol. B **33**, 883 (2002).
[19] U. Tengblad, TSL/ISV Report No. 96-0163, 1996 (unpublished).
[20] CERN Program Library Long Write-up W5013, GEANT-Detector Description and Simulation Tool.
[21] Particle Data Group, K. Hagiwara *et al.*, Phys. Rev. D **66**, 010001 (2002).
[22] A. M. Green, J. A. Niskanen, and S. Wycech, Phys. Rev. C **54**, 1970 (1996); S. Wycech and A. M. Green, *ibid.* **64**, 045206 (2001).
[23] N. V. Shevchenko *et al.*, Phys. Rev. C **58**, R3055 (1998).
[24] N. V. Shevchenko *et al.*, Eur. Phys. J. A **9**, 143 (2000).
[25] A. Deloff, Phys. Rev. C **61**, 024004 (2000).
[26] H. Garcilazo and M. T. Peña, Phys. Rev. C **61**, 064010 (2000); H. Garcilazo, *ibid.* **67**, 067001 (2003).
[27] A. Fix and H. Arenhövel, Eur. Phys. J. A **9**, 119 (2000); Nucl. Phys. **A697**, 277 (2002).
[28] M. Batinić, I. Šlaus, and A. Švarc, Phys. Rev. C **52**, 2188 (1995).
[29] B. L. Birbrair and A. B. Gridnev, Z. Phys. A: Hadrons Nucl. **354**, 95 (1996).
[30] A. M. Green and S. Wycech, Phys. Rev. C **60**, 035208 (1999).
[31] M. Lacombe *et al.*, Phys. Lett. **101B**, 139 (1981).